

# In vivo measurement of mid-infrared light scattering from human skin

Anna P. M. Michel,<sup>1,2,\*</sup> Sabbir Liakat,<sup>3</sup> Kevin Bors,<sup>3</sup> and Claire F. Gmachl<sup>1,3</sup>

<sup>1</sup>Princeton Institute for the Science and Technology of Materials, Princeton University, Princeton, NJ 08540, USA

<sup>2</sup>Current Address: Department of Applied Ocean Physics and Engineering, Woods Hole Oceanographic Institution, Woods Hole, MA 02543, USA

<sup>3</sup>Department of Electrical Engineering, Princeton University, Princeton, NJ 08540, USA  
\*[apmichel@princeton.edu](mailto:apmichel@princeton.edu)

**Abstract:** Two mid-infrared light sources, a broadband source from a Fourier Transform Infrared Spectrometer (FTIR) and a pulsed Quantum Cascade (QC) Laser, are used to measure angle-resolved backscattering in vivo from human skin across a broad spectral range. Scattering profiles measured using the FTIR suggest limited penetration of the light into the skin, with most of the light interacting with the stratum corneum layer of the epidermis. Scattering profiles from the QC laser show modulation patterns with angle suggesting interaction with scattering centers in the skin. The scattering is attributed to interaction of the laser light with components such as collagen fibers and capillaries in the dermis layer of the skin.

© 2013 Optical Society of America

**OCIS codes:** (290.5820) Scattering measurements; (140.5965) Semiconductor lasers, quantum cascade; (170.6930) Tissue.

## References and links

1. H. H. Mantsch and D. Chapman, eds., *Infrared Spectroscopy of Biomolecules* (Wiley-Liss, 1996).
2. L. Wang and B. Mizaikoff, "Application of multivariate data analysis techniques to biomedical diagnostics based on mid-infrared spectroscopy," *Anal. Bioanal. Chem.* **391**, 1641–1654 (2008).
3. R. Bhargava, "Infrared spectroscopic imaging: the next generation," *Appl. Spectrosc.* **66**, 1091–1120 (2012).
4. R. Mendelsohn, C. R. Flach, and D. J. Moore, "Determination of molecular conformation and permeation in skin via IR spectroscopy, microscopy, and imaging," *Biochim. Biophys. Acta* **1758**, 923–933 (2006).
5. A. P. M. Michel, S. Liakat, E. Zanghi, K. Ostrander, and C. F. Gmachl, in *The 11th International Conference on Intersubband Transitions and Quantum Wells (ITQW)*, Badesi, Italy (Sept. 12, 2011).
6. V. Tuchin, *Handbook of Optical Sensing of Glucose in Biological Fluids and Tissues* (CRC Press, Taylor and Francis, 2008).
7. S. N. Thennadil, J. L. Rennert, B. J. Wenzel, K. H. Hazen, T. L. Ruchti, and M. B. Block "Comparison of glucose concentration in interstitial fluid, and capillary and venous blood during rapid changes in blood glucose levels," *Diabetes Technol. Ther.* **3**, 357–365 (2001).
8. J. M. Schmitt and G. Kumar, "Optical scattering properties of soft tissue: a discrete particle model," *Appl. Opt.* **37**, 2788–2797 (1998).
9. L. V. Wang and H. Wu, *Biomedical Optics: Principles and Imaging* (Wiley-Interscience, 2007).
10. J. R. Mourant, J. P. Freyer, A. H. Hielscher, A. A. Eick, D. Shen, and T. M. Johnson, "Mechanisms of light scattering from biological cells relevant to noninvasive optical-tissue diagnostics," *Appl. Opt.* **37**, 3586–3593 (1998).
11. A. N. Bashkatov, E. A. Genina, V. I. Kochubey, and V. V. Tuchin, "Optical properties of human skin, subcutaneous and mucous tissues in the wavelength range from 400 to 2000 nm," *J. Phys. D: Appl. Phys.* **38**, 2543–2555 (2005).
12. S. Liakat, A. P. M. Michel, K. Bors, and C. F. Gmachl, "Mid-infrared ( $\lambda=8.4\text{--}9.9\mu\text{m}$ ) light scattering from porcine tissue," *Appl. Phys. Lett.* **101**, 093705 (2012).

13. R. Kong and R. Bhargava, "Characterization of porcine skin as a model for human skin studies using infrared spectroscopic imaging," *Analyst* **136**, 2359–2366 (2011).
  14. "American National Standard for Safe Use of Lasers," ANSI Standard Z136.1-2007 (R2007).
  15. A. Krishnaswamy and G. Baranoski, "A biophysically based spectral model of light interaction with human skin," *Comput. Graph. Forum* **23**, 331–340 (2004).
  16. R. R. Anderson and J. A. Parrish, "The optics of human skin," *J. Invest. Dermatol.* **77**, 13–19 (1981).
  17. N. Kollias and G. Stamatias, "Optical non-invasive approaches to diagnosis of skin diseases," *J. Invest. Dermatol. Symp. Proc.* **7**, 64–75 (2002).
  18. A. Vogel and V. Venugopalan, "Mechanisms of pulsed laser ablation of biological tissues," *Chem. Rev.* **103**, 577–644 (2003).
  19. I. S. Saidi, S. L. Jacques, and F. K. Tittel, "Mie and Rayleigh modeling of visible-light scattering in neonatal skin," *Appl. Opt.* **34**, 7410–7418 (1995).
  20. R. R. Anderson and J. A. Parrish, "Optical properties of human skin," in *The Science of Photomedicine*, J. A. Parrish and J. F. Regan, eds. (Plenum, New York, 1982), pp. 147–194.
  21. V. Tuchin, *Tissue Optics: Light Scattering Methods and Instruments for Medical Diagnosis*, 2nd ed. (SPIE Press, 2007).
- 

## 1. Introduction

The mid-infrared (mid-IR) spectral range ( $\sim 3 - 30 \mu\text{m}$ ) shows promise for a range of biomedical applications and is of interest for pharmaceutical applications due to the strong, yet spectrally distinct, absorption features exhibited here by several biomarkers (e.g. glucose, proteins, lipids, and urea) [1, 2]. By taking advantage of such features and through an understanding of skin and mid-IR light interactions, novel non-invasive, pain-free optical sensors for monitoring will be realized. Infrared techniques such as infrared spectroscopic imaging which couples an infrared light source with an optical microscope can provide extensive information about tissue samples [3]. Such approaches include Fourier transform infrared spectroscopic imaging which couples an interferometer with an IR microscope and an array detector and discrete frequency infrared (DF-IR) spectroscopic imaging [3]. These imaging techniques have bio-optical applications including tissue classification. Spatially resolved infrared spectra of tissue can provide insight into molecular composition and physiological function. Examining how spectra vary with depth through tissue can provide information about the structure of skin [4].

One disease that would greatly benefit from the development of a non-invasive optical sensor is diabetes. The development of an optical glucose sensor that takes advantage of the molecule's mid-IR absorption features in the  $8.6 \mu\text{m}$  to  $9.6 \mu\text{m}$  region [5] would allow diabetics to monitor glucose levels without the need of a finger prick. Non-invasive monitoring has the potential to eliminate possible exposure to blood-borne pathogens and to increase monitoring compliance through pain-free sensing. Further it introduces the possibility to make sensors that can continuously measure glucose levels. Such continuous monitoring would contribute to the better maintenance of blood sugar levels and aid in the prevention of diabetic shock. A range of optical techniques and approaches have been or are currently being explored for non-invasive or minimally-invasive glucose detection and an in depth examination of the topic is covered by Tuchin [6]. Although current glucose monitors measure blood glucose levels, optical sensing could instead target the interstitial fluid in the dermis layer and correlate its glucose concentration to that in the blood [7]. Glucose is present in the interstitial fluid layer at concentrations less than that in blood. Demonstration that mid-IR light can penetrate into the dermis layer of the skin is the key first step for developing an optical sensor that can measure glucose within the interstitial fluid.

Optical differences exist in skin due to spatial variability of the refractive index [8]. Since the refractive index of tissue is not uniform (varies between approximately 1.34 to 1.62) both between tissue layers (e.g. epidermis, dermis) and within these layers, light scatters within the skin [9]. Each layer of skin has different scattering properties which depend on particle size, type, and density. For example, scattering centers include cells and both their organelles

and organelle structures [10]. The outer layer, the epidermis, has two layers, the 20  $\mu\text{m}$  thick stratum corneum non-living layer and the living epidermis (about 100  $\mu\text{m}$  thick) layer which contains the melanin. Below the epidermis is the stronger scattering layer, the dermis ( $\sim 1 - 4$  mm thick). The scattering property of the dermis is primarily due to the collagen fibrils packed into collagen bundles. Light scatters from both single fibrils and scattering centers resulting from the interlacement of collagen fibrils with bundles [11].

Through the use of Quantum Cascade (QC) lasers, mid-IR sources that are capable of producing high peak power pulses with low average power, we explore the capability to use mid-IR radiation to reach the dermis layer of human skin *in vivo*. Previous work by our group has shown the ability to penetrate *ex vivo* into the dermis layer of porcine skin with a QC laser [12]. Here we focus on human *in vivo* measurements and use both a Fourier transform infrared spectrometer and a QC laser as a source for investigating infrared light interactions with skin. We demonstrate the ability to reach the dermis layer *in vivo*, in human skin with mid-IR light through measurement of backscattered light.

## 2. Materials and methods

Two infrared sources, a broadband source from a ThermoFisher Fourier Transform Infrared Spectrometer (FTIR) or a widely-tunable external cavity Daylight Solutions Inc. Quantum Cascade Laser (EC-QC laser), were combined with a liquid nitrogen-cooled MCT (HgCdTe) detector attached to a motion-controlled bi-axial rotation device (BARD) (Fig. 1) to measure angle-resolved light interactions with skin. A flip-mounted mirror enabled the BARD to be used with either light source without the need for realignment of the optical beam path. The FTIR provides a broadband source of approximately 600 - 8000  $\text{cm}^{-1}$  while the EC-QC laser provides a tunable pulsed source from 990 - 1225  $\text{cm}^{-1}$  (8.2 - 10.1  $\mu\text{m}$ ). Through the use of the spectral sources that cover a range of wavelengths, we investigate wavelength dependence on scattering. Broad spectral coverage also has application to glucose sensor development due to its broad spectral features in the mid-IR.

In this work, light interactions with human skin (*in vivo*) samples were studied. These studies were approved by the Princeton University Institutional Review Board. Measurements on ethnically diverse human subjects were made on the inner arm with human consent obtained from all subjects. Full angular resolved data were taken on three subjects of Caucasian, African American, and Asian ethnicities. For human skin measurements, FTIR spectra were taken using a resolution of 4  $\text{cm}^{-1}$ ; yet, the scans were limited to 5 per angle measured (from 20° to 100°) to minimize the time the human subjects' arms were positioned for experiments (20 minutes). High gain (8) and a large aperture (150) were needed due to the low light scattering levels measured on the detector resulting from the low output power of the FTIR (estimated to be  $\sim 7$  mW total from the FTIR integrated across the full spectral range). *Ex vivo* porcine samples were also analyzed using FTIR spectroscopy with spectra taken using a resolution of 4  $\text{cm}^{-1}$  with 20 scans per angle measured. Porcine skin samples were frozen and then thawed for several hours prior to experimentation. Kong and Bhargava have previously shown the stability of porcine skin samples over multiple days at room temperature, shown relative consistency among different samples, and demonstrated the similarities of porcine skin to human skin both structurally and chemically. Kong and Bhargava affirm the appropriateness of using porcine skin as a proxy for human skin for spectroscopic studies [13]. Although experiments by Kong and Bhargava look at the spectral features in porcine skin, these studies do not focus on measuring scattered light. The EC-QC laser was operated in pulsed mode (100 kHz, 500 ns pulses, 100 mW peak power). By operating in pulsed mode, we keep the average power low, at levels well below the threshold that a subject could sense the incident beam, a key requirement for a non-invasive medical sensor. Minimizing average power avoids possible thermal damage to the skin or ab-

lation while maintaining high peak power allows for light collection scattered from deep in the skin. The ANSI standard [14] requires that the maximum permissible exposure (MPE) for skin exposure to a laser beam in the  $9\ \mu\text{m}$  region to be  $100\ \text{mW}/\text{cm}^{-2}$ . We remain well below this MPE at an estimated value of  $70\ \text{mW}/\text{cm}^{-2}$ .

Use of the BARD setup allows for precise control of both the incident angle ( $\phi$ ) by sample rotation and the detector collection angle ( $\theta$ ) (Fig. 1). A lens is used to focus the incoming light onto the sample and two lenses are used for focusing the scattered light onto the detector. For EC-QC laser measurements, a custom LabView program was used to automate the motion controller, to tune the EC-QC laser, and to record the detector signal via a National Instruments data acquisition board. The external detector was interfaced directly with the FTIR for broadband measurements.

Detector alignment was repeated for each individual skin sample with no realignment made between angular changes. To align the detector, a sanded (rough surface) aluminum plate was placed on the sample holder and  $\phi$  and  $\theta$  were set to the specular angle  $30^\circ$  and  $60^\circ$  respectively. The detector signal was maximized by changing the x-y-z position of the detector. Correlation of the measured voltage on the detector with actual optical power (mW) on the detector was determined using an Ophir II power meter and a polarizer for varying incoming power levels. For power measurement data, the QC laser output was set to  $1120\ \text{cm}^{-1}$ .

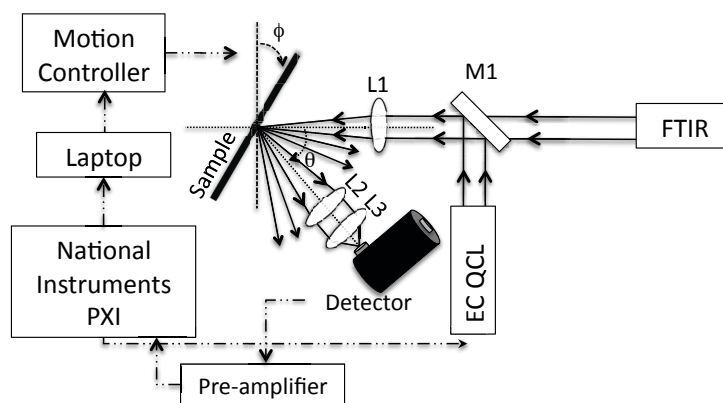


Fig. 1. Schematic drawing of the experimental setup. A mirror (M1) was attached to a flip mount to allow for either source, the FTIR or the EC-QCL, to be used without realignment of the optical beam path. A lens (L1) was used to focus the collimated light onto the sample. Two lenses (L2 and L3) were used to collect the scattered light from the skin onto the detector.

### 3. Results and discussion

FTIR spectroscopy was used to examine light-skin interactions across a broad spectral range. Figures 2 and 3 show two representative measurements for ex vivo porcine skin samples and in vivo human samples, respectively. Both skin types show mid-IR light scattering patterns with a maxima close to, though somewhat offset from the specular angle. Both show strong scattering in the  $2000 - 3000\ \text{cm}^{-1}$  region, with porcine skin showing a much broader spectral range of strong scattering. In the area of interest for glucose sensing, close to  $1000\ \text{cm}^{-1}$ , we

see a significant scattering signal in the angular-resolved data. The full-width-half-maximum (FWHM) for the human skin is  $32.5^\circ$  (measured at  $2500\text{ cm}^{-1}$ ) whereas the FWHM for porcine skin is  $50^\circ$  at the same wavenumber. A range of factors could contribute to this. For example, the porcine skin is *ex vivo* and was previously frozen whereas the human skin is *in vivo*, which introduces differences in sample hydration, physical stability of the sample in the beam path, and levels of surface lipids.

Typically about 5 - 7 % of light incident on the stratum corneum is reflected back. The stratum corneum, though thin, is not smooth and planar and contains folds, the extent of which is sample dependent, which causes the reflectance off skin to not be specular [15, 16]. These folds result in a beam of collimated incident radiation passing through the stratum corneum to be refracted and become more diffuse [16]. The light is diffusely reflected more if the folds are more extensive. The broad maxima present suggest that we are not collecting specular reflections and instead are measuring diffuse reflections. However, the depth of light penetration into the skin is low with the light reaching only the epidermis, which we have previously seen for porcine skin [12].

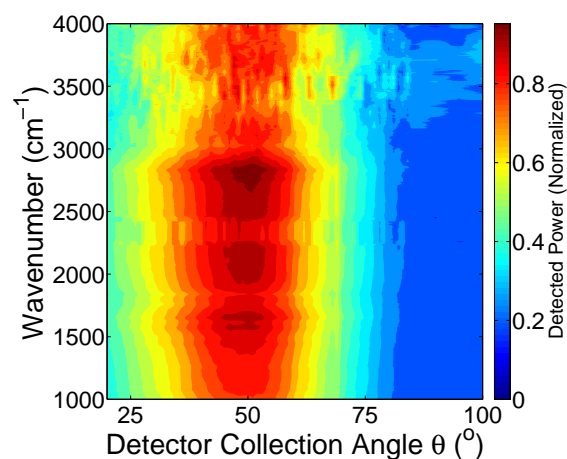


Fig. 2. Measurement of infrared light interaction with porcine skin using FTIR spectroscopy ( $\phi = 30^\circ$ ).

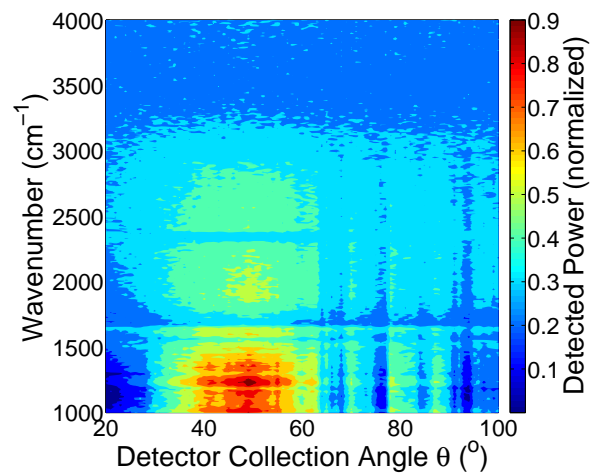


Fig. 3. Measurement of infrared light interaction with human skin in vivo using FTIR spectroscopy ( $\phi = 30^\circ$ ).

Figure 4 shows an example reflection spectrum of human skin using the FTIR, taken here at  $\theta = 50^\circ$  in lab air. The principal absorbing species in skin in the mid-IR region is water (OH band, seen in the  $3400\text{ cm}^{-1}$  range) which is attributable to stratum corneum hydration. Many of the spectral features typically seen using FTIR for skin measurements are those belonging to water, due to such hydration [21]. Stratum corneum lipids result in absorption peaks in the  $2800\text{-}3000\text{ cm}^{-1}$  range, though these are very weakly seen in our data. The spectral feature at  $1170\text{ cm}^{-1}$  can be attributed to an ester C-O asymmetric stretch [13]. Amide I and II bands are also present close to  $1545$  and  $1655\text{ cm}^{-1}$  [13, 17]. Sebaceous lipids exhibit absorption peaks in the  $1700\text{ cm}^{-1}$  range [17]. From examination of the peaks present, we see mostly interaction from the water and surface lipids. This suggests the depth of penetration using the broadband light is limited and supports the conclusion that most of our mid-IR light is being scattered off the stratum corneum or penetrating only weakly into the epidermis. In order to use mid-IR radiation to detect glucose within the dermis layer, infrared light must penetrate deeper into the skin; thus we explore the use of higher powered pulses of infrared light from a QC laser.

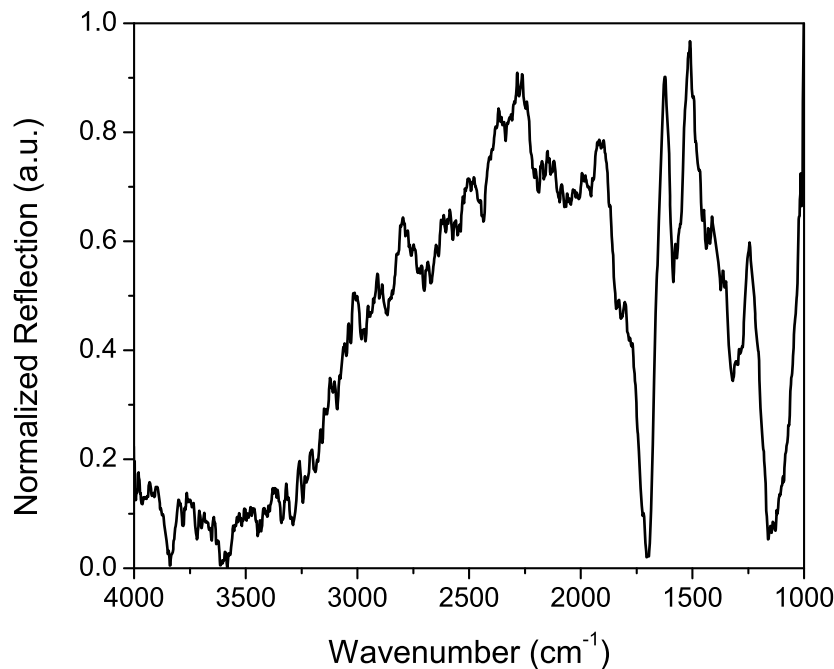


Fig. 4. FTIR spectrum of reflection by human skin.

Figure 5 shows a representative plot of the QC laser light interaction with human skin. Distinct angular modulations are present, suggesting that scattering off scattering centers within the tissue is taking place. Unlike the data shown above using FTIR, the uniform peak intensity centered close to the specular angle of  $60^\circ$  is non-existent. This suggests that instead of the dominant reflections and scattering off the stratum corneum, that the QC light is penetrating the tissue deeper than the FTIR broadband source. Figure 6 shows data from three human subjects, examining the detected power compared to the input power with the QC laser tuned to  $1120\text{ cm}^{-1}$ . This wavenumber was selected for being highly representative of the intensities meas-

ured across a broad span of angles in Fig. 5. The power measured is again not symmetric about the specular angle. Approximately 100 mW of input power is needed to measure on the order of  $10 \mu\text{W}$  on the detector. Similar incident power requirements were previously measured in our group for porcine skin samples [12]. Peak intensities are not uniform across angles with the maximum detected power ( $25 \mu\text{W}$ ) appearing at random locations throughout the plots. These locations correspond to scattering centers within the skin, such as those from collagen with the dermis layer, that the incoming light interacts with [12].

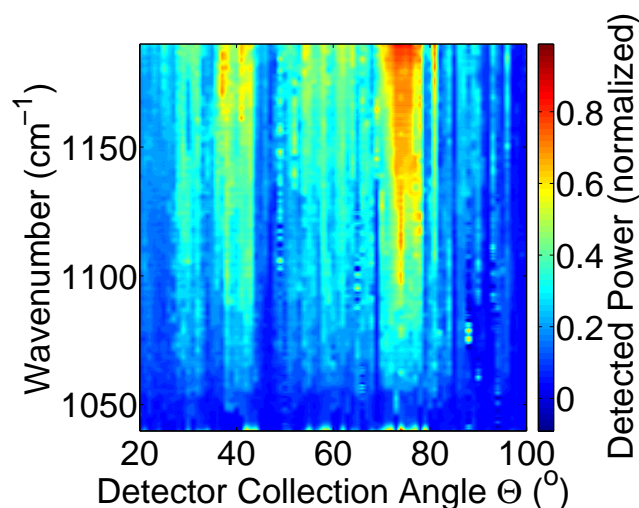


Fig. 5. Measurement of infrared light interaction with human skin using a QC laser source.

When light penetrates the dermis, it can be absorbed and scattered, with diffuse backscattering occurring [15]. The dermis is highly light scattering due to its high collagen content. The dermis layer's function is to protect underlying tissue and organs from injury and exhibits both elastic deformability and high strength due to the collagen. The dry weight of dermis is composed of about 75% collagen. Within the dermis layer are collagen fibers with diameters of  $1 - 10 \mu\text{m}$  [18]. Collagen fibers are wavy, forming a non woven network, and are composed of individual fibrils embedded in a matrix which has a high water content. Collagen fibers are strong scatterers and are the primary scatterer in skin [19]. Collagen fibers are present in the dermis in many orientations, though typically aligned parallel to the skin surface. However, since scattered light in tissue is diffuse, light interacts with the collagen fibers at a range of angles. The extent of scattering of normal incident light by a collagen fiber depends on wavelength, fiber diameters, and the differences in indices of refraction between the actual fibers and their surrounding matrix [19]. Scattering of light by particles suspended in a medium, such as that of skin, can be described by Rayleigh and Mie scattering. Rayleigh scattering occurs when particles are much smaller than the wavelength and Mie scattering occurs when particles are on the same order as the wavelength [19]. Most skin light scattering is caused by particles, specifically collagen fibers of the same size as the wavelength of the light [20]. The wavelength of the QC laser light is on a similar scale to the size of collagen fibers. Rayleigh scattering occurs from the organelles; yet, the total backscattered light is a combination of Rayleigh scattering and reflections from the collagen. The reflections are dependent on the angle the collagen is oriented; thus, it is suggested that the modulation patterns seen result from scattering off collagen in the dermis. The randomness of the location of the scattering sites seen and the lack of a distinct intense peak around the specular angle supports this. The strong scattering nature



of the collagen in the dermis layer as compared to the epidermal layer, thus suggests that the QC light is penetrating into the dermis layer, which we have seen previously through in depth studies using porcine skin [12]. Additional scattering and thus additional variability present in the plots may result from the surfaces of the stratum corneum, interfaces within the tissue, and other scattering centers in the dermis. Further variability in data may result from speckle structure formation resulting when coherent light is passed through a scattering medium [21]. At 8.6 - 9.6  $\mu\text{m}$ , the absorption coefficient is estimated to be approximately 200 - 230  $\text{cm}^{-1}$  with significant absorption in this region due to water [21]. An estimation of the reduced scattering coefficient [ $\mu'_s = \mu_s(1-g)$ , where  $g$  is the anisotropy factor of scattering] can be made through using a power law,  $\mu'_s(\lambda) = a\lambda^{-w}$ , where  $\lambda$  is wavelength in nanometers. Bashkatov et al. present values of  $a = 73.7$  and  $w = .22$  for Mie scattering in the 400 to 2000 nm region for human skin in vitro. When these values are extrapolated to the mid-infrared region and an anisotropy factor of 0.9 is assumed and applied to 8.6 - 9.6  $\mu\text{m}$ , this results in a  $\mu'_s(\text{Mie}) = 9.8 - 10 \text{ cm}^{-1}$ . The Rayleigh scattering can be estimated using  $\mu'_s(\text{Rayleigh}) = b \lambda^{-4}$  with  $b$  estimated to be  $1.1 \times 10^{12}$ . Thus we estimate for 8.6 - 9.6  $\mu\text{m}$  that  $\mu'_s(\text{Rayleigh}) = 1.3 \times 10^{-4}$  to  $2.0 \times 10^{-4}$  [11].

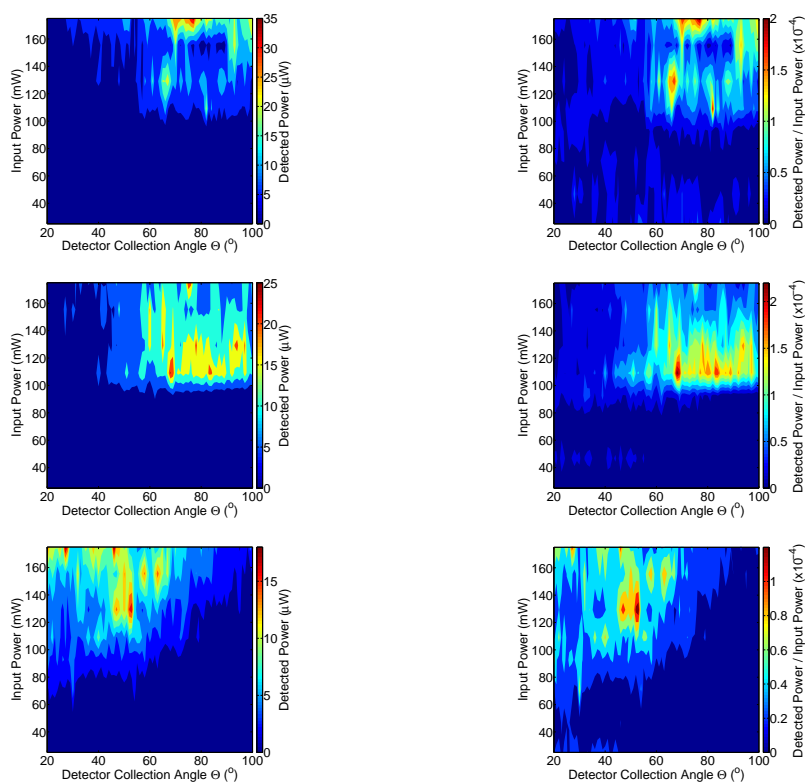


Fig. 6. The left column from top-to-bottom shows detected power (mW) on three different human subjects. The right column from top-to-bottom shows detected power normalized to input power for the same three human subjects.

Melanin, found in the stratum corneum and epidermis in both human and porcine skin results in skin pigmentation [16]. At wavelengths longer than about 1.1  $\mu\text{m}$  however, there is no significant absorption by melanin [16]. Anderson et al. demonstrated that in studies of the

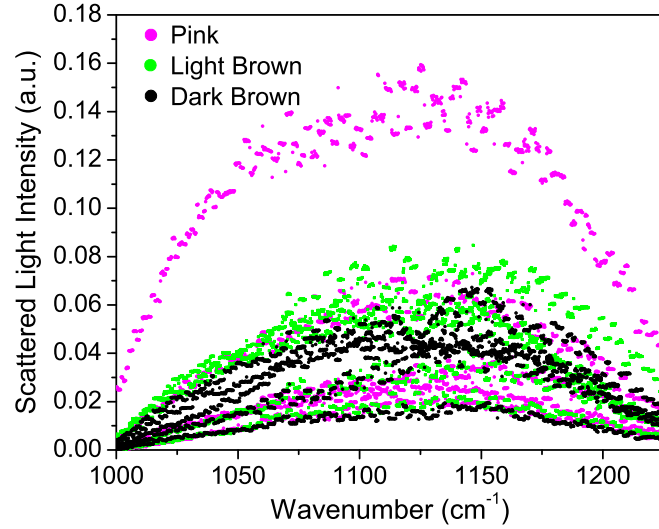


Fig. 7. Scattered light intensity collected from porcine skin with three different melanin contents.

UV-visible-near infrared spectrum, penetration of the dermis is greater at longer wavelengths [16]. Through the use of three different pigmented porcine samples (pink, light brown, and dark brown) all taken from juvenile pigs, we compared spectral intensities across the tuning range of the QC laser (Fig. 7) to verify that the skin pigmentation does not influence our measurements. Sample thicknesses were measured to eliminate the possibility that irregularities in thickness contributed to the intensities measured. We saw no appreciable spectral differences due to sample color, suggesting that scattering is much more complex than variability due to pigmentation can explain. In the development of an optical glucose sensor for human use in which the light must penetrate to the dermal layer, it is important that skin characteristics, such as pigmentation, do not affect the measurement techniques.

#### **4. Conclusion**

Optical sensing has the potential to be used for non-invasive, pain-free monitoring of glucose. Interstitial fluid in the dermis layer of the skin contains glucose that can be used as a proxy for blood glucose levels. In order to reach the dermis layer, light must penetrate the epidermis, including the outer stratum corneum layer. Furthermore, to measure the glucose in the dermis layer, the light must not only interact with the interstitial fluid, but must also be backscattered from the dermis layer at detectable levels. The signal and intensity of the light collected must then be correlated to the glucose levels. Although measurements made with a broadband infrared source (FTIR) showed the distinct spectral signature of skin, the light interacted primarily with the stratum corneum layer and was confined to the epidermis. This was attributed to the low input power of the source. The use of a QC laser with 100 mW peak power and 5 mW average power demonstrated the ability to penetrate deeper into the human skin by using high peak power pulses. Angularly-resolved modulation patterns are attributed to interaction of the light with collagen scattering centers in the dermis layer. Future work will thus focus on the detection of glucose contained in the dermis layer using QC laser light.

#### **Acknowledgments**

The authors acknowledge Daylight Solutions Inc. for their assistance with the QC laser. The authors acknowledge the MIRTHE Center, NSF-ERC Grant EEC-0540832 and the Eric and Wendy Schmidt Transformative Technology Fund.